УДК 551.465

©*А. Г. Лучинин*, *М. Ю. Кириллин*
©Перевод *Е. С. Кочеткова*, 2019
Институт прикладной физики РАН, г. Нижний Новгород
luch@appl.sci-nnov.ru

МОДЕЛИРОВАНИЕ РАСПРОСТРАНЕНИЯ СЛОЖНО МОДУЛИРОВАННОГО СВЕТОВОГО ИМПУЛЬСА В МОРСКОЙ ВОДЕ

Статья поступила в редакцию 13.05.2019, после доработки 18.09.2019

Исследованы характеристики распространяющегося в воде светового импульса, модулированного радиосигналом с линейно изменяющейся во времени частотой. Анализ выполнен на основе статистического моделирования импульсных и частотных характеристик сигнала и аналитического представления сигнала в виде импульса, описываемого функцией Гаусса с внутриимпульсной модуляцией. Оценены изменения времени прихода и длительности огибающей импульса, вызванные разбросом фотонов по путям пробега при расстояниях между источником и приемником до четырех глубин видимости белого диска. Показано, что эти изменения могут иметь разные знаки в зависимости от частотного диапазона модуляции. Выполнено сравнение времен прихода и длительности импульса с меняющейся во времени частотой и импульса после согласованной обработки – свертки с копией модулирующего сигнала. Показано, что в исследованном диапазоне изменения параметров многократное рассеяние не препятствует сжатию сложного сигнала при его согласованной обработке.

Ключевые слова: подводная оптическая связь, сложные сигналы, волны фотонной плотности, временная дисперсия, согласованная обработка, Монте-Карло моделирование.

A. G. Luchinin, M. Yu. Kirillin
Institute of Applied Physics RAS, Nizhny Novgorod, Russia

SIMULATION OF COMPLEXLY MODULATED LIGHT PULSE PROPAGATION IN SEA WATER

Received 13.05.2019, in final form 18.09.2019

The characteristics of a light pulse propagating in water modulated by a radio signal with a frequency varying linearly with time are investigated. The analysis is based on statistical modeling of the pulse and frequency characteristics of the signal and the analytical representation of the signal as a pulsedescribed by a Gaussian function with intrapulse modulation. Changes in the arrival time and the pulse envelope duration caused by the photon pathlength dispersion at distances between the source and receiver up to four white disk visibility depths are estimated. It is shown that these changes may have different signs depending on the modulation frequency range . A comparison was made between arrival times and durations of the pulse with a time-varying frequency and the pulse after matched processing consisting in convolution with the original modulating signal. It is shown that in the investigated range of parameter changes, multiple scattering does not prevent the compression of a complex signal when it is matched processing.

Key words: underwater optical communication, complex signals, photon density waves, temporal dispersion, matched processing, Monte Carlo simulation.

Multiple scattering of light in water is an essential factor of the spatio-temporal structure formation of the light field from artificial sources. This factor, along with the absorption of light in water, limits the resolution and range of underwater vision systems and the range of communication through an optical underwater (wireless) channel. In addition to the energy attenuation of the signal during its propagation from the radiation source (transmitter) to the receiver, multiple scattering due to the spread of photons along the paths leads to distortion

Ссылка для цитирования: *Лучинин А.Г.*, *Кириллин М.Ю.* Моделирование распространения сложно модулированного светового импульса в морской воде // Фундаментальная и прикладная гидрофизика. 2019. Т. 12, № 4. С. 66–77.
For citation: *Luchinin A.G.*, *Kirillin M.Yu.* Simulation of complexly modulated light pulse propagation in sea water. *Fundamentalnaya i Prikladnaya Gidrofizika*. 2019, 12, 4, 66–77.
DOI: 10.7868/S2073667319040087

of its shape and an additional delay due the photon pathlength dispersion. These effects are most noticeable for typical signal variation times, comparable with the time of mean free path of photons in water, and can limit the information transfer speed even at relatively short distances. An estimate of their magnitude can be performed by having a numerical or analytical representation of the pulse transfer function for the system "emitter – water (signal propagation path) – receiver". Obviously, the transfer function must comprise the characteristics of modulation and demodulation of the emitted and received signal. An alternative approach to the system description can be based on the use of complex frequency response. This characteristic directly describes the complex transfer coefficient when modulating a continuous radiation source by a harmonic signal of a given frequency and can be used to calculate the transmission coefficients of signals with any given modulation (as does a pulse transition function). Temporal dispersion caused by photon multiple scattering leads to the frequency dependence of the attenuation coefficient of the harmonics that form the signal. In addition, phase distortions of the signal arise due to the frequency dependence of the phase and group velocities of photon density waves corresponding to these spectral harmonics. The effect of multiple scattering on the properties of the variable component of the optical field at high modulation frequencies (the so-called photon density wave) in various analytical approximations and based on statistical Monte Carlo simulation was discussed in [1—17]. An experimental study of this problem is presented in a list of research [18—22]. At the same time, the properties of light fields excited in a scattering medium by sources, which power is modulated by complex high-frequency signals, have not been practically studied. An exception is a study [23], in which, based on the Monte Carlo method and an approximate analytical description, the properties of a lidar signal with linear frequency modulation were investigated. The present work aims at revealing the features of the complex modulated signals propagation in seawater as applied to an underwater (wireless) optical communication channel. Based on the signal model proposed in [23], changes' estimates of the signal arrival time and its duration due to multiple light scattering in water are obtained.

1. The problem formulation and description of the model

We assume that the radiation source has infinitely small spatial-angular dimensions and its radiance can be written in the form:

$$L_S(z=0,\mathbf{n},t)=\delta(\mathbf{r}_\perp)\delta(\mathbf{n}-\mathbf{z}_0)P_S(t), \tag{1}$$

where z and $\mathbf{r}_\perp$ are coordinates describing the position of a point in space, $\mathbf{n}$ is a unit vector describing the direction of the beam, t is time, δ is the delta function for the corresponding variables, $\mathbf{z}_0$ is a unit vector in the z axis direction of the Cartesian coordinate system, function $P_S(t)$ describes the change in time of the radiation power and is normalized: $\int P_S(t)dt=W$, where W is a total pulse energy. We also assume that the receiver has a circular aperture located on the axis of the initial radiation beam with coordinates $\mathbf{r}_\perp=0$, z and its direction pattern that is isotropic in a hemisphere facing the radiation source. Then the radiation power supplied to the photodetector can be expresses as:

$$P_R(t)=\iint\limits_{\Sigma} E(\mathbf{r}_\perp,z,t)d\mathbf{r}_\perp, \tag{2}$$

where

$$E(\mathbf{r}_\perp,z,t)=\iint\limits_{n_z\geq 0} L(\mathbf{r}_\perp,z,\mathbf{n},t)(\mathbf{n}\mathbf{z}_0)d\mathbf{n} \tag{3}$$

represents the spatial-temporal distribution of the irradiation created by the source (1) over a plane surface $z=const$, n_z is a vector $\mathbf{n}$ projection on the axis z and $L(\mathbf{r}_\perp,z,\mathbf{n},t)$ is a field radiance in the medium. Further we introduce the spectral representations of functions $P_{S,R}(t)$:

$$P_{S,R}(\omega)=\frac{1}{2\pi}\int P_{S,R}(t)\exp(-i\omega t)dt \tag{4}$$

Due to the linearity of the problem, the relation:

$$P_R(\omega,z)=F_S^0(\omega)F_w(\omega,z), \tag{5}$$

where $F_S^0(\omega)$ describes the spectral composition of the emitted signal, and $F_w(\omega,z)$ there is a complex transfer coefficient of the spectral harmonic of the frequency ω from the emitter to the receiver with spatial-angular characteristics specified (1) and (2), (3). Further, it is convenient to present the function $F_S^0(\omega)$ as a sum $F_S^0(\omega)=\overline{F_S^0}(\omega)+\widetilde{F_S^0}(\omega)$, where the first and second terms correspond to the low-frequency and high-frequency parts of the spectrum, respectively. Suppose that after the photodetector in the receiving path, the high-frequency component of the signal is filtered and processed further. Then, to calculate the spectral power of the high-frequency part of the photocathode normalized signal $\widetilde{P_R}(\omega,z)$, equation (5) assumes the form:

$$\widetilde{P_R}(\omega,z)=\widetilde{F_S^0}(\omega)F_w(\omega,z)\widetilde{F_R^0}(\omega), \tag{6}$$

where $\widetilde{F_R^0}(\omega)$ is a frequency response of the processing path of the high-frequency part of the signal. Suppose that the receiving path provides processing consistent with the signal modulating the emitted light pulse. With this processing, with the accuracy of the constant coefficients

$$\widetilde{F_R^0}(\omega)=\left(\widetilde{F_S^0}(\omega)\right)^* \text{ and } \widetilde{F_S^0}(\omega)\widetilde{F_R^0}(\omega)=\left|\widetilde{F_S^0}(\omega)\right|^2.$$

Complex frequency transfer coefficient $F_w(\omega,z)$ can be calculated based on the results of Monte Carlo simulations of the pulse transfer function for the source power set in the form of a delta function in time and the subsequent fast Fourier transform. This modeling approach, as applied to the calculation of the pulsed and frequency characteristics of a light beam in seawater, was described in [19]. Presenting the function $F_S^0(\omega)$ as required, this approach allows calculation of the characteristics of complex signals.

To evaluate the nature and magnitude of the effects caused by the photon pathlength dispertion in water and its effect on the characteristics of the radiation reaching the receiver, we specify the form of the pulses, restricting ourselves to intrapulse modulation with a linearly varying frequency of the modulating signal. Let the radiation source generate a Gaussian pulse with a mean square duration t_0. The power of this pulse is given by the formula:

$$P_S(t)=\frac{W}{2t_0\sqrt{2\pi}}\exp\left(-\frac{t^2}{2t_0^2}\right)\left(1+m\cdot\cos(\omega_0+\beta t)t\right), \tag{7}$$

where m is a modulation depth, ω_0 is a modulation frequency center, β is a rate of frequency change. from (4) and (7) follows the expression for the emitted signal spectrum in the positive frequencies range:

$$F_S^0(\omega)=\frac{W_0}{4\pi}\left(\exp\left(-\frac{\omega^2t_0^2}{2}\right)+\frac{m\alpha_0}{\sqrt{2}}\exp\left(-(\omega-\omega_0)^2\alpha_0^2t_0^2\right)\right). \tag{8}$$

Here $\alpha_0^2=\left(2(1-iB)\right)^{-1}$, and $B=t_0\Delta\omega=2\beta t_0^2$ is a modulating signal base, and $\Delta\omega=2\beta t_0$ is an effective bandwidth of the modulation. The second term in (8) describes the high-frequency component of the emitted pulse (function $\widetilde{F_S^0}(\omega)$), which must be distinguished during signal processing. Therefore, expression (6) for the signal power spectrum after matching processing can be represented as:

$$\widetilde{P_R}(\omega,z)=\frac{A}{\sqrt{1+B^2}}\exp\left(-\frac{(\omega-\omega_0)^2t_0^2}{1+B^2}\right)F_w(\omega,z). \tag{9}$$

Coefficient A, to reduce the recording, includes constant factors characterizing the level of radiation and parameters of the receiving system that are not essential for the problem under consideration.

From (9) it follows the known in radio and sonar detection fact that the problem of the propagation of a pulse modulated by a high-frequency signal with a linearly varying frequency is reduced to the problem of the pulse propagation modulated by a harmonic signal with a frequency ω_0, and duration inversely proportional to the original complex signal base (for $B>>1$). Further, to simplify the analysis and following [23], an approximate representation of the frequency transfer coefficient is used:

$$F_W(\omega,z)=\Phi(\omega,z)\exp\left(-i\frac{\omega z}{c}+i\varphi(\omega,z)\right), \tag{10}$$

$$\varphi(\omega,z)=\varphi(\omega_0,z)+\varphi'(\omega-\omega_0)+\frac{1}{2}\varphi''(\omega-\omega_0)^2, \tag{11}$$

$$\Phi(\omega,z)=\Phi(\omega_0,z)\exp\left(\Psi'(\omega-\omega_0)+\frac{1}{2}\Psi''(\omega-\omega_0)^2\right). \tag{12}$$

The following notation were introduced in (10)—(12): $\Phi(\omega,z)=\left|F_W(\omega,z)\right|$, $\varphi(\omega,z)$ is an additive to the geometric phase incursion due to multiple scattering in water, *c is* the speed of light in water, $\varphi'=\left.\frac{\partial\varphi(\omega,z)}{\partial\omega}\right|_{\omega=\omega_0}$ $\varphi''=\left.\frac{\partial^2\varphi(\omega,z)}{\partial\omega^2}\right|_{\omega=\omega_0}$, $\Psi'=\left.\frac{\partial\left(\ln\left(\Phi(\omega,z)\right)\right)}{\partial\omega}\right|_{\omega=\omega_0}$, $\Psi''=\left.\frac{\partial^2\left(\ln\left(\Phi(\omega,z)\right)\right)}{\partial\omega^2}\right|_{\omega=\omega_0}$. Of course, the possibility of using expansion (11), (12) is very limited, therefore, for specific estimates, it is necessary to control the fulfillment of inequations:

$$\frac{\Psi''B^2}{2\ln\left(\Phi(\omega,z)\right)t_0^2}\ll 1,\ \frac{\varphi''B^2}{\varphi t_0^2}\ll 1. \tag{13}$$

In view of (10)—(12), expression (9) assumes the form:

$$P_R(\omega,z)=\frac{A\Phi(z,\omega_0)}{\sqrt{1+B^2}}\exp\left(\left(i\left(\varphi_b'-\frac{z}{c}\right)+\Psi'\right)(\omega-\omega_0)-Q_0(\omega-\omega_0)^2\right), \tag{14}$$

where $Q_0=\frac{t_0^2}{1+B^2}-\frac{\Psi''+i\varphi''}{2}$, φ_b is the additional phase delay due to multiple scattering in water. The expression for the time dependence of the shape of the high-frequency component of the pulse detected by the receiving system directly follows from (14):

$$P(t,z)=\frac{A\Phi(z,\omega_0)\sqrt{\pi}}{\sqrt{Q_0\left(1+B^2\right)}}\exp\left(i\omega_0 t-\frac{\left(\varphi_b'-\frac{z}{c}-i\Psi'+t\right)^2}{4Q_0}\right). \tag{15}$$

Considering the approximations used, formulas (14), (15) exhaustively describe the spectral composition and time characteristics of a pulse for given characteristics of the propagation path and the properties of the emitter and receiver. Function $\Phi(z,\omega_0)$ describes the attenuation of the signal, while its derivatives represent changes in the arrival time and pulse width caused by multiple scattering. From (15), we can obtain expressions for the averagearrival time of the center of gravity of the envelope of the high-frequency component:

$$\overline{t}=\frac{z}{c}-\varphi_b'+\frac{\mathrm{Im}(Q_0)\Psi'}{\mathrm{Re}(Q_0)}. \tag{16}$$

The third term in (16) results from the frequency dependence of the signal attenuation. When the emitted signal base is equal to or close to zero, its value is negligible. From (15), also follows the expression for the mean square duration of the envelope of the echo signal that has undergone matched processing:

$$\sqrt{\overline{\Delta t_0^{\,2}}} = \sqrt{2\left(\mathrm{Re}\, Q_0^{-1}\right)^{-1}}\,. \tag{17}$$

Additionally, note that similar parameters of the high-frequency component of the pulse arriving at the photodetector (which did not undergo the matched processing) are also described by formulas (16), (17), but with the replacement of the parameter Q_0 with Q_1:

$$Q_1 = \frac{t_0^2}{2(1+iB)} - \frac{\Psi'' + i\varphi''}{2}\,. \tag{18}$$

The estimation of the pulse parameters that are not collapsed with the standard pulse can be of independent interest, both in a range of applications and for a clear understanding of the physical phenomena that affect the propagation of signals with a finite modulation band.

2. Monte Carlo simulation and frequency transfer coefficient

For the impulse transfer function simulation, the original code was used, in which the indicatrix of seawater scattering is integrated. The technique and modeling features are described in [15—17]. As a modeling result and for further spectral dependences calculations we used the ratio:

$$K\left(\mathbf{r}_{0\perp}, z, t_k\right) = \frac{\overline{E\left(\mathbf{r}_{0\perp}, z, t_k\right)}}{W}\,.$$

Function $K\left(\mathbf{r}_{0\perp}, z, t_k\right)$ represents the transfer coefficient of energy transferred through the area ΔS during the time interval $(t_k, t_k + \Delta t)$, t_k is the current time, $\overline{E\left(\mathbf{r}_{0\perp}, z, t\right)} = \iint\limits_{\Delta S} E\left(\mathbf{r}_{\perp}, z, t\right) d\mathbf{r}_{\perp}$, $\mathbf{r}_{0\perp}$ determines the position of the receiving aperture relative to the axis of the beam. Here, with a few exceptions, we restrict ourselves to the case when the center of the circular receiving aperture with radius R is situated on the axis.

In terms of the Monte Carlo technique, the coefficient $K\left(\mathbf{r}_{0\perp}, z, t_k\right)$ represents the ratio of the number of photons intercepted by the aperture $\Delta S = \pi R^2$ during Δt, to the number of photons released at a point $\mathbf{r} = 0$ at time $t = 0$ in the direction $n_z = 1$. For optical communication channel applications, it can be interpreted as a pulsed transfer function (pulsed transfer coefficient) for the spatial and angular characteristics of the source and receiver specified above. Applying to the function $K\left(\mathbf{r}_{0\perp}, z, t_k\right)$ fast Fourier transform procedure over a discrete variable t_k, the complex frequency transfer coefficient of the water layer between the source and receiver can be calculated, as a function of the discrete frequency: $F_W\left(\omega_n, z\right)$.

The function $K\left(\mathbf{r}_{0\perp}, z, t_k\right)$ and $F_W\left(\omega_n, z\right)$ behavior with increasing distance between the source and the receiver was studied in detail in [17]. For the purposes of this work, optical distances at which a noticeable effect of time dispersion on the structure of complex modulated signals can be expected are of the greatest interest. As preliminary estimates show, significant changes in the duration of the high-frequency component of the modulated pulse occur, starting from distances exceeding $1.5z_б - 2z_б$ ($z_б$ – Secchi depth). On the other hand, distances exceeding $5z_б - 6z_б$, become unavailable for Monte Carlo modeling, because they require too much computing resources. (Note that for the function $K\left(\mathbf{r}_{0\perp}, z, t_k\right)$ modeling for one of the possible problem parameters' combinations up to 1012 photons were used). Therefore, here, we confine ourselves to a range of distances from 45 to120 meters with a fixed set of optical water characteristics. The properties of the medium were set by the magnitude of the primary optical characteristics, namely, scattering coefficient, true absorption coefficient, and scattering indicatrix. A typical marine scattering indicatrix was used in the calculations. $X(\theta)$, obtained by Yu.E. Ochakovsky (quoted by [24]) and extrapolated to the angles 0° and 180° (fig. 1). The mean scattering cosine of the indicatrix is 0.931.

The values of the scattering and absorption coefficients of water were set equal to 0.16 1/m and 0.04 1/m, which corresponds to a photon survival probability of 0.8.

The time-averaging interval was 10^{-11} s. Fig. 2 and 3 present the functions calculated based on statistical modeling $K(\mathbf{r}_{0\perp}, z, t_k)$ and fast Fourier transform frequency dependencies of functions $\ln(\Phi(f,z))$ and $\varphi(f,z)$, where $f = (2\pi)^{-1}\omega$. The inlay to fig. 2 shows the distance dependence of the function $\ln(\Phi(f=0,z))$ under the normalization condition $\Phi(f=0,z) = \int_{-\infty}^{\infty} K(\mathbf{r}_{0\perp}, z, t)dt$. Note that under this condition the function $F_W(f,z)$ means a complex transfer coefficient with a stationary source modulated by a harmonic signal with a frequency *f*.

As follows from the form of the plots, the greatest dependence of the decrement of the photon density waves on the frequency is observed at frequencies greater than 107 Hz, moreover, the greater the distance z, the stronger is this dependence. A similar character is observed for the phase (dispersion) characteristics of these waves.

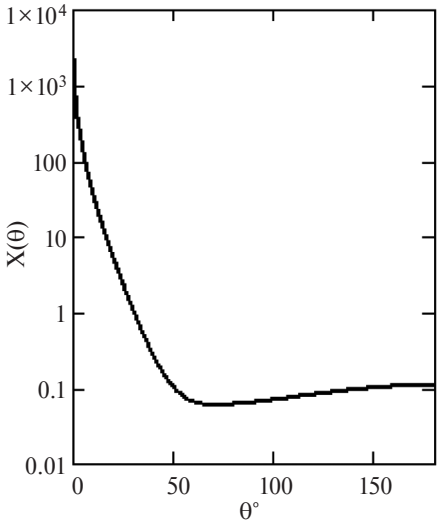

Fig. 1. Scattering phase function.

Рис. 1. Индикатриса рассеяния морской воды.

At frequencies greater than 10^9 Hz, the decrement is determined mainly by the unscattered component of the radiation (ballistic photons) and practically does not depend on the frequency, and an additional phase delay $\varphi(f,z)$ tends to zero. Therefore, specifically in the range of modulation frequencies 10^7—10^9 Hz a change in the structure of the pulse with broadband modulation is expected. In this context, the region of frequencies and distances at which the attenuation and phase delay reach a maximum corresponding to a minimum in the frequency characteristics is of particular interest, see fig. 2 and fig. 3. The formation of this minimum, as shown in [17], is associated with the splitting of the pulse transfer function on the beam axis and the appearance of the second maximum pulse formed by multiple scattering lagging behind the head (determined by ballistic

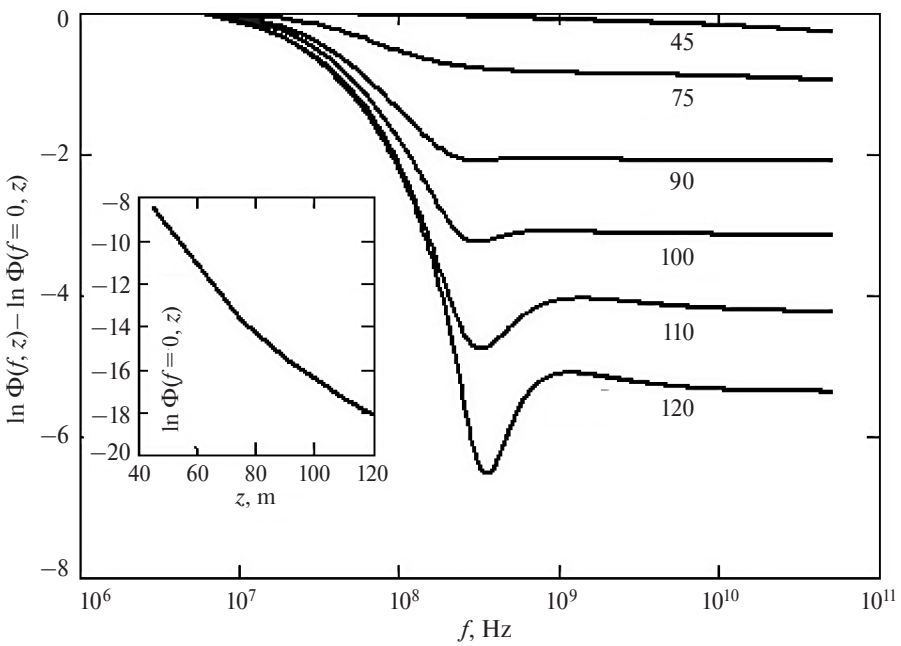

Fig. 2. Frequency response $\Phi(f,z)$ at different distances *z* between the source and receiver (numbers at the curves in meters).

Рис. 2. Амплитудно-частотная характеристика $\Phi(f,z)$ при различных расстояниях z между источником и приемником (цифры у кривых в метрах).

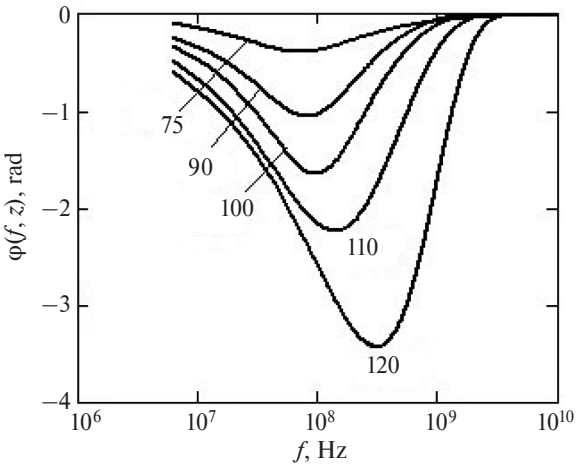

Fig. 3. Phase response $\varphi(f,z)$ at different distances between the source and receiver z (numbers at the curves in meters).

Рис. 3. Фазово-частотная характеристика $\varphi(f,z)$ при различных расстояниях между источником и приемником z (цифры у кривых в метрах).

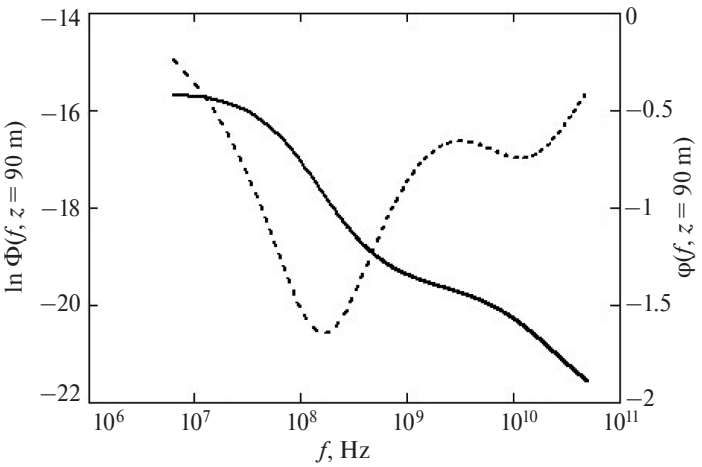

Fig. 4. Frequency and phase responses at a distance of 90 m from the source by $r_{0\perp} = 0.25$ m (solid and dashed curve, respectively).

Рис. 4. Амплитудно-частотные и фазово-частотные характеристики при $r_{0\perp} = 0.25$ м на расстоянии 90 м от источника (сплошная и пунктирная кривая соответственно).

photons). As will be shown below, this effect can lead to a change in the signs of "delay" and a relative change in the duration of the high-frequency component of the modulated pulse.

It should be emphasized once again that the data shown in fig. 2 and 3, refer to the case of the receiver location strictly on the axis of the beam. in the case of its displacement, when the ballistic photons do not fall on the receiving aperture and do not participate in the formation of the signal, the frequency response takes on a qualitatively different form. As an example, we give here the amplitude-frequency and phase-frequency characteristics when the center of the receiving aperture is displaced by a distance $r_{0\perp} = 0.25$ m from the beam axis at a 90 m distance from the emitter (fig. 3).

3. Impulse delay

Further, the change in the arrival time of the pulse associated with multiple scattering $\overline{\Delta t} = \overline{t} - z/c$ is estimated. For clarity, the parameters of the initial pulse are set: its duration and the deviation of the modulating signal. Let the base of the modulating signal B be equal to ten, and the pulse duration determined by the value of the central modulation frequency be $t_0 = 10/f_0$. We also introduce the relative change in the arrival time $\overline{\delta t} = \overline{\Delta t}/t_0$. This parameter calculation results for a pulse that has not undergone matched processing and a compressed pulse is shown in fig. 5 and 6.

Note the main features of the parameter $\overline{\delta t}$ variability. As expected, its greatest variability is observed in the frequency range with maximum dispersion. Deviations of this parameter from zero increase with increasing z, which is also to be expected. Non-trivial is negative $\overline{\delta t}$ in a certain range of modulation frequencies. This fact was noted earlier in the study of the dispersion properties of photon density waves in the case of the self-similar approximation [14] and is explained by the redistribution of the modulation depth inside the pulse as it propagates deep into the medium. Spectral harmonics with lower frequencies are attenuated less than high-frequency ones, therefore the center of gravity of the envelope of the pulse variable component is shifted towards the front edge. The effect is reversed in the region of large distances and frequencies, where the amplitude-frequency characteristic has a minimum. Note that when the sign of β changes, graphs of fig. 5 are inverted relative to the value $\overline{\delta t} = 0$, which confirms the nature of the negative parameter values $\overline{\delta t}$. As can be seen from fig. 5, negative value $\overline{\delta t}$ can reach half the pulse duration even with a relatively small bandwidth of the modulating signal. The

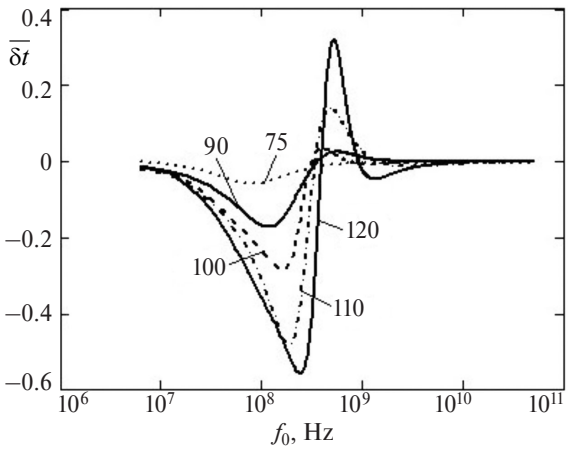

Fig. 5. The relative change of the arrival time of an unprocessed pulse versus of the center modulation frequency at different distances between the source and receiver (numbers on the curves).

Рис. 5. Относительное изменение времени прихода не обработанного импульса как функция центральной частоты модуляции при различных расстояниях между источником и приемником (цифры у кривых).

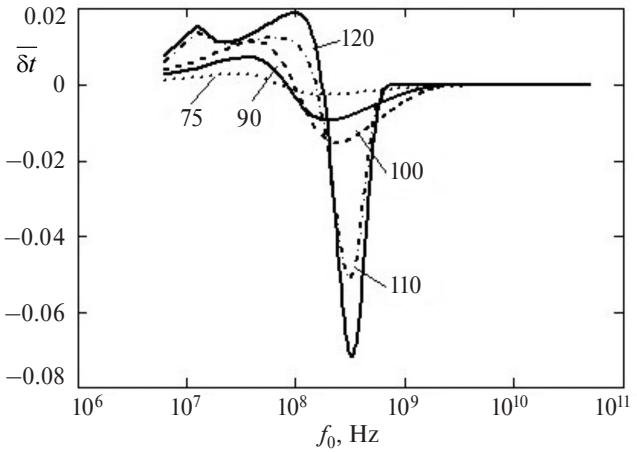

Fig. 6. The same as in fig. 4 for a pulse after matched processing (i.e. for a compressed pulse).

Рис. 6. То же, что и на рис. 4 для импульса после согласованной обработки (т.е. для сжатого импульса).

advance towards broadband modulation, where B >> 10, for distances $z \geq 75$, considering the accepted approximations, is not possible due to violations of conditions (13). Frequency dependence of the parameter $\overline{\delta t}$, calculated similarly for a compressed pulse, is presented in fig. 6. The changes in absolute value $\overline{\delta t}$ in the studied region of the problem parameters, are significantly lower than for the unprocessed pulse. As for the dependence of the value on the central modulation frequency, it is, ultimately, also related to the finite width of the compressed pulse $\Delta f = (t_0)^{-1}\sqrt{1+B^2}$ and, as a result, to the frequency dependence of the attenuation coefficient and the phase of spectral harmonics.

Similar relationships between the delay values of these pulses' types are observed when the receiver is shifted from the beam axis. Fig. 7 shows the frequency dependence of the relative delay $\overline{\delta t}$, calculated for a combination of parameters fig. 4. Also, note a qualitative difference from the plots in fig. 5 and 6, which manifests itself in the

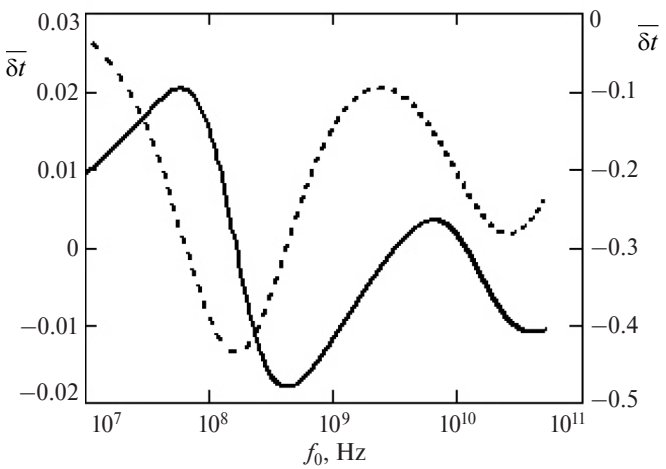

Fig. 7. Relative change of the arrival time of a compressed (solid curve, left ordinate axis) and not processed pulse (dashed line, right ordinate axis) versus of the central modulation frequency at $z = 90$ m and $r_{0\perp} = 0.25$ m.

Рис. 7. Относительное изменение времени прихода сжатого (сплошная кривая, левая ось ординат) и не обработанного импульса (пунктир, правая ось ординат) как функция центральной частоты модуляции при $z = 90$ м и $r_{0\perp} = 0.25$ м.

absence of asymptotics at high values of the modulation frequency, which is associated with the formation of the signal only by scattered (non-ballistic) photons.

4. Change the pulse width

Let us introduce the normalized signal durations, $\Delta\tau_0 = \frac{\sqrt{\overline{\Delta t_0{}^2}\left(1+B^2\right)}}{t_0}$, $\Delta\tau_1 = \frac{\sqrt{\overline{\Delta t_1{}^2}}}{t_0}$, where $\overline{\Delta t_0^2}$ is set by (17), and $\overline{\Delta t_1^2}$ by the same equation with the replacement from Q_0 to Q_1, corresponding to an unprocessed pulse Frequency dependences of normalized signal durations for the same set of parameters as for fig. 5 and 6 are presented in fig. 8. The greatest variability is experienced by signals in the frequency range from 10^8—10^9 Hz. In

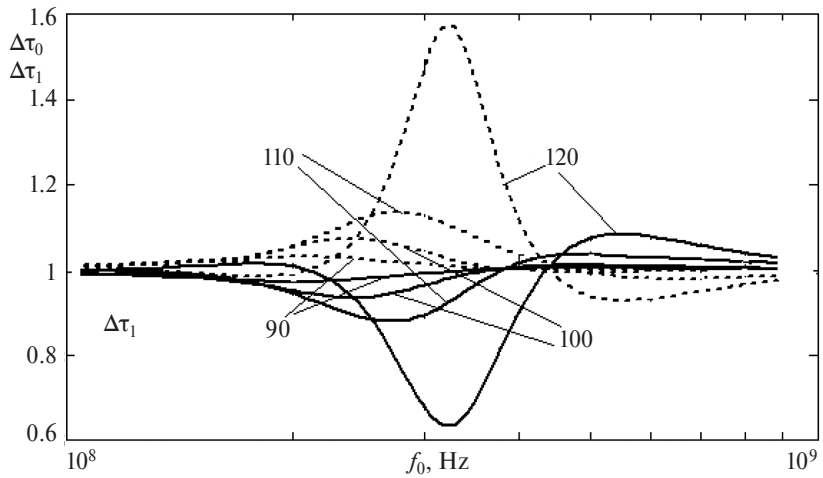

Fig. 8. Changes in the signal versus function of the central modulation frequency at different distances between the source and receiver (numbers on the curves). The solid curves were calculated for pulses that underwent matched processing, and dashed curves – for raw pulses.

Рис. 8. Изменение длительности сигнала как функция центральной частоты модуляции при различных расстояниях между источником и приемником (цифры у кривых). Сплошные кривые рассчитаны для импульсов, прошедших согласованную обработку, штриховые – для необработанных импульсов.

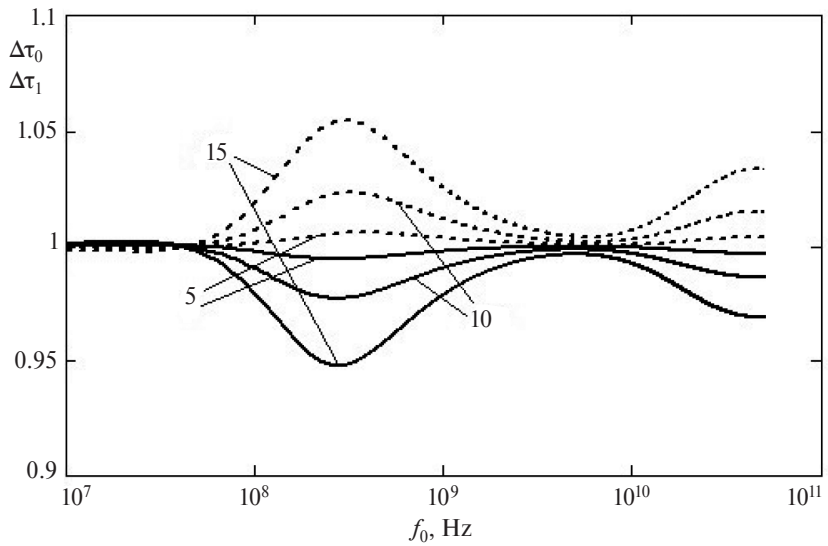

Fig. 9. The relative change of the duration of the compressed (*solid curves*) and non-processed pulse (*dashed line*) versus a function of the center modulation frequency at $z = 90$ m, $r_{0\perp} = 0.25$ m and various base values.

Рис. 9. Относительное изменение длительности сжатого (*сплошные кривые*) и не обработанного импульса (*пунктир*) как функция центральной частоты модуляции при $z = 90$ м, $r_{0\perp} = 0.25$ м и различных значениях базы.

most of this range, a signal that has undergone matched processing undergoes additional compression, while an unprocessed signal undergoes additional broadening. As follows from fig. 8, the role of these effects increases with distance z. Noteworthy is the fact that the sign of these changes at the edges of the range changes. Such a nontrivial behavior of the frequency dependences of the pulse duration change under the effect of multiple scattering is apparently caused by a specific form of the frequency characteristic $F_W(f,z)$ and, as a consequence, by the difference in attenuation and by phase delays of the spectral harmonics that form the signal.

Qualitatively different frequency dependencies of the parameters $\Delta\tau_0$ and $\Delta\tau_1$ can be expected when the receiver is shifted away from the beam axis. This is primarily due to the expansion of the region of significant change of function $F_W(f,z)$ towards high frequencies and the type of phase-frequency characteristic (in particular, the appearance of a second minimum in an additional phase delay). As a result, the second region of a noticeable change in the pulse duration is formed, shifted toward the maximum limits for the modulation frequencies modeling. Fig. 9 shows parameter changes $\Delta\tau_0$ and $\Delta\tau_1$ for the same conditions as for fig. 7, for various base values of the modulating signal.

5. Conclusion

The presented analysis was performed for a very limited, although typical set of parameters describing the propagation path of optical pulses underwater and modulation/demodulation approaches. Therefore, it can serve only as an example and the basis of a relatively simple estimation of possible distortions of transmitted signals caused by multiple scattering. Nevertheless, these results can be extended to other combinations of scattering and absorption water parameters with the same probability of photon survival and the same scattering phase function. In that case, the scales of spatial, temporal, and frequency variables should be changed following the principle of physical similarity.

The main conclusion that can be drawn from the obtained results is that scattering in water practically does not impede the matched processing of complex signals, at least in the studied range of distances and modulation bands. This result is not entirely trivial since multiple scattering in water can significantly distort the initial phase, and amplitude ratios of harmonics forming a complex signal. In this regard, it seems important in the future to expand the limits of the resented approximations and evaluate the possible distortions of the transmitted signals with a significantly larger modulation band ($B >> 1$) and in media with a different degree of scattering anisotropy.

The authors are grateful to L.S. Dolin for attention to work and useful discussions.

This study was supported by the Russian Foundation for Basic Research (project 19-02-0089) and by the State project "Development of radiophysical methods for ocean research" (0035-2019-0006).

Литература

1. *Лучинин А.Г.*, *Савельев В.А.* О распространении синусоидально модулированного светового пучка в рассеивающей среде // Изв. Вузов. Радиофизика. 1969. Т. 12, № 2. С. 256—262.
2. *Лучинин А.Г.*, *Савельев В.А.* Асимптотика синусоидально модулированного излучения в изотропно рассеивающей среде // Изв. Вузов. Радиофизика. 1970. Т. 13, № 12. С. 1789—1793.
3. *Кацев И.Л.* О глубинном режиме при распространении в мутной среде синусоидально модулированного пучка света // Изв. АН СССР. Физика атмосферы и океана. 1971. Т. 8, № 2. С. 212—216.
4. *Лучинин А.Г.* О пространственной структуре синусоидально модулированного пучка света в среде с сильно анизотропным рассеянием // Изв. Вузов. Радиофизика. 1971. Т. 14, № 12. С. 1925—1927.
5. *Лучинин А.Г.* Пространственный спектр узкого синусоидально модулированного пучка света в анизотропно рассеивающей среде // Изв. АН СССР. Физика атмосферы и океана. 1974. Т. 10, № 12. С. 1312—1317.
6. *Ремизович В.С.*, *Рогозкин Д.Б.*, *Рязанов М.И.* Распространение узкого модулированного пучка света в рассеивающей среде с учетом флуктуаций путей фотонов при многократном рассеянии // Изв. Вузов. Радиофизика. 1982. Т. 25, № 8. С. 891—898.
7. *Mullen L.*, *Laux A.*, *Concannon B.*, *Zege E.P.*, *Katsev I.L.*, *Prikhach A.S.* Amplitude-Modulated Laser Imager // Applied Optics. 2004. V. 43. P. 3874—3892.
8. *Zege E.P.*, *Katsev I.L.*, *Prikhach A.S.*, *Mullen L.J.* Simulating the performance of in-water modulated vision systems with estimation of the image quality characteristics // Proceedings of the International Conference on Current Problems in Optics of Natural Waters (ONW'2005). Saint-Petersburg, D.S. Rozhdestvensky Optical Society, 2005. P. 312—320.

9. *Luchinin A.G.* Concept of an oceanological lidar with maximal 3D resolution // Proceedinds of VI International conference "Current problems in optics of natural waters". Saint-Petersburg: Nauka, 2011. P. 37—43.
10. *Лучинин А.Г.* Теория подводного лидара со сложно модулированным пучком подсветки // Известия РАН. Физика атмосферы и океана. 2012. Т. 48, №6. С. 739—748.
11. *Лучинин А.Г.* О системах подводного видения со сложно модулированными пучками подсветки // Фундаментальная и прикладная гидрофизика. 2012. Т. 5, № 4. С. 5—17.
12. *Лучинин А.Г.*, *Долин Л.С.* Модель системы подводного видения со сложно модулированным пучком подсветки // Известия РАН. Физика атмосферы и океана. 2014. Т. 50, № 4. С. 468—476.
13. *Лучинин А.Г.*, *Долин Л.С.* Применение сложно модулированных волн фотонной плотности для инструментального видения в мутных средах // Докл. АН. Физика. 2014. Т. 455, № 6. С. 643—646.
14. *Лучинин А.Г.*, *Долин Л.С.* О дисперсионных свойствах волн фотонной плотности в анизотропно рассеивающих средах // Изв. ВУЗов. Радиофизика. 2016. Т. 59, № 2. С. 162—170.
15. *Лучинин А.Г.*, *Кириллин М.Ю.* Структура модулированного узкого пучка света в морской воде: моделирование методом Монте-Карло // Известия РАН. Физика атмосферы и океана. 2017. Т. 53, № 2. С. 275—284.
16. *Luchinin A.G.*, *Kirillin M.Yu.*, *Dolin L.S.* Backscatter signal in underwater lidars: temporal and frequency features // Appl. Opt. 2018. V. 57. P. 673—677.
17. *Luchinin A.G.*, *Kirillin M.Yu.* Temporal and frequency characteristics of a narrow light beam in sea water // Applied Optics. 2016. V. 55. P. 7756—7762.
18. *Гордеев Л.Б.*, *Лучинин А.Г.*, *Щегольков Ю.Б.* Экспериментальные исследования структуры узкого синусоидально модулированного пучка света в модельной анизотропно рассеивающей среде // Изв. АН СССР. Физика атмосферы и океана. 1975. Т. 1, № 1. С. 86—89.
19. *Mullen L.*, *Laux A.*, *Concannon B.*, *Zege E.P.*, *Katsev I.L.*, *Prikhach A.S.* Demodulation techniques for the amplitude modulated laser imager // Applied Optics. 2007. V. 46. P. 7374—7383.
20. *Cochenour B.*, *Mullen L.*, *Muth J.* Modulated pulse laser with pseudorandom coding capabilities for underwater ranging, detection, and imaging // Applied Optics. 2011. V. 50. P. 6168—6178.
21. *Mullen L.*, *Lee R.*, *Nash J.* Digital passband processing of wideband-modulated optical signals for enhanced underwater imaging // Applied Optics. 2016. V. 55(31). C18—C24.
22. *Bartolini L.*, *De Dominicis L.*, *de Collibus M.F.*, *Fornetti G.*, *Guarneri M.*, *Paglia E.*, *Poggi C.*, *Ricci R.* Underwater three-dimensional imaging with an amplitude-modulated laser radar at a 405 nm wavelength // Applied Optics. 2005. V. 44(33). P. 7130—7135.
23. *Luchinin A.G.*, *Dolin L.S.*, *Kirillin M.Yu.* Time dispersion delay and width variation of complex modulated signal in underwater lidar // Applied Optics. 2019. V. 58. P. 5074—5085.
24. *Иванов А.* Введение в океанографию. М.: Мир, 1978. 574 с.

References

1. *Luchinin A.G.*, *Savel'ev V.A.* Propagation of a sinusoidally modulated light beam through a scattering medium. *Radiophysics and Quantum Electronics*. 1969, 12, 2, 205—211.
2. *Luchinin A.G.*, *Savel'ev V.A.* The asymptotic behavior of a sinusoidally modulated radiation field in an isotropically scattering medium. *Radiophysics and Quantum Electronics*. 1970, 13, 12, 1378—1382.
3. *Katzev I.L.* The asymptotic regime in the deep layers of scattering medium illuminated by sinusoidally modulated light beam. *Izv.Acad. Sci. USSR Atmos. Oceanic Phys*. 1971, 7, 2, 212—218.
4. *Luchinin A.G.* The spatial structure of a sinusoidally modulated light beam in a medium having strongly anisotropic scattering. *Radiophysics and Quantum Electronics*. 1971, 14, 1507—1509.
5. *Luchinin A.G.* Spatial spectrum of a narrow sine-wave-modulated light beam in an anisotropically scattering medium. *Izv. Acad. Sci. USSR Atmos. Oceanic Phys*. 1974, 10, 12, 1312—1317.
6. *Remizovich V.S.*, *Rogozkin D.B.*, *Ryazanov M.I.* Propagation of a narrow modulated light beam in a scattering medium with fluctuations of the photon pathlengths in multiple scattering. *Radiophysics and Quantum Electronics*. 1982, 25, 639—646.
7. *Mullen L.*, *Laux A.*, *Concannon B.*, *Zege E.P.*, *Katsev I.L.*, *Prikhach A.S.* Amplitude-Modulated Laser Imager. *Applied Optics*. 2004, 43, 3874—3892.
8. *Zege E.P.*, *Katsev I.L.*, *Prikhach A.S.*, *Mullen L.J.* Simulating the performance of in-water modulated vision systems with estimation of the image quality characteristics. *Proceedings of the International Conference on Current Problems in Optics of Natural Waters (ONW'2005)*. *Saint-Petersburg*, *D.S. Rozhdestvensky Optical Society*, 2005, 312—320.
9. *Luchinin A.G.* Concept of an oceanological lidar with maximal 3D resolution. *Proceedinds of VI International conference* "*Current problems in optics of natural waters*". Saint-Petersburg, Nauka, 2011, 37—43.
10. *Luchinin A.G.* Theory of underwater lidar with a complex modulated illumination beam. *Izvestiya*. *Atmospheric and Oceanic Physics*. 2012, 48, 6, 663—671.

11. *Luchinin A.G.* On Underwater Imaging Systems with Complex Modulated Beams of Illumination. *Fundamentalnaya i Prikladnaya Gidrofizika*. 2012, 5, 4, 5—17 (in Russian).
12. *Luchinin A.G.*, *Dolin L.S.* Model of an underwater imaging system with a complexly modulated illumination beam. *Izvestiya. Atmospheric and Oceanic Physics*. 2014, 50, 4, 411—419.
13. *Luchinin A.G.*, *Dolin L.S.* Application of complex-modulated waves of photon density for instrumental vision in turbid media. *Doklady Physics*. 2014, 59, 4, 170—172.
14. *Luchinin A.G.*, *Dolin L.S.* On dispersive properties of the photon-density waves in an anisotropic scattering medium. *Radiophysics and Quantum Electronics*. 2016, 59, 2, 145—152.
15. *Luchinin A.G.*, *Kirillin M.Yu.* Structure of a modulated narrow light beam in seawater: Monte Carlo simulation. *Izvestiya. Atmospheric and Oceanic Physics*. 2017, 53, 2, 242—249.
16. *Luchinin A.G.*, *Kirillin M.Yu.*, *Dolin L.S.* Backscatter signal in underwater lidars: temporal and frequency features. *Appl. Opt*. 2018, 57, 673—677.
17. *Luchinin A.G.*, *Kirillin M.Yu.* Temporal and frequency characteristics of a narrow light beam in sea water. *Applied Optics*. 2016, 55, 7756—7762.
18. *Gordeev L.B.*, *Luchinin A.G.*, *Shcegol'kov Yu.B.* Experimental studies of the structure of a narrow sine-wave-modulated light beam in a model anisotropically scattering medium. *Izv. Atmos. Ocean. Phys*. 1975, 11, 50—53.
19. *Mullen L.*, *Laux A.*, *Concannon B.*, *Zege E.P.*, *Katsev I.L.*, *Prikhach A.S.* Demodulation techniques for the amplitude modulated laser imager. *Applied Optics*. 2007, 46, 7374—7383.
20. *Cochenour B.*, *Mullen L.*, *Muth J.* Modulated pulse laser with pseudorandom coding capabilities for underwater ranging, detection, and imaging. *Applied Optics*. 2011, 50, 6168—6178.
21. *Mullen L.*, *Lee R.*, *Nash J.* Digital passband processing of wideband-modulated optical signals for enhanced underwater imaging. *Applied Optics*. 2016, **55**(31), C18—C24.
22. *Bartolini L.*, *De Dominicis L.*, *de Collibus M.F.*, *Fornetti G.*, *Guarneri M.*, *Paglia E.*, *Poggi C.*, *Ricci R.* Underwater three-dimensional imaging with an amplitude-modulated laser radar at a 405 nm wavelength. *Applied Optics*. 2005, **44**(33), 7130—7135.
23. *Luchinin A.G.*, *Dolin L.S.*, *Kirillin M.Yu.* Time dispersion delay and width variation of complex modulated signal in underwater lidar. *Applied Optics*. 2019, 58.